THE ASTROPHYSICAL JOURNAL, 279:1–12, 1984 April 1


# ALIGNMENTS OF CLUSTERS OF GALAXIES AS A PROBE FOR SUPERCLUSTERS

AVISHAI DEKEL,[1,2] MICHAEL J. WEST,[1] AND SVERRE J. AARSETH[3]
*Received 1983 July 11; accepted 1983 September 2*

## ABSTRACT

We use *N*-body simulations of competing cosmological scenarios to study the relative orientations of the principal axes of clusters of galaxies and the lines connecting them to neighboring clusters and find that they provide a sensitive test for the formation of the large-scale structure in the universe. The observed tendency of clusters to point toward each other reflects the existence of 20–50 Mpc $h^{-1}$ *elongated* superclusters that construct a large-scale cell structure. Tidal interactions between clusters are found *not* to produce similar alignments, presumably because the clusters are surrounded by underdense regions. Hence the scenario in which superclusters have collapsed from excessive fluctuations on large scales is favored over hierarchical clustering from fluctuations on smaller scales. Rich clusters (but not necessarily galaxies) had to be formed after, or during, the aspherical collapse of superclusters, i.e., not long before $z \sim 1$.

Other tests are applied to the simulated samples: the axial ratios of clusters on various scales are found to be sensitive to the elongation of superclusters, while the maximum percolation length is less sensitive to it here.

*Subject headings:* cosmology — galaxies: clustering — galaxies: formation

## I. INTRODUCTION

A basic difference between the major scenarios for the formation of structure in the universe is expected to show up in the *shapes* of the large-scale structures, as has been pointed out by Zel'dovich, Einasto, and Shandarin (1982). In the scenario (hereafter the I scenario) where the structure on all scales evolves from small to large scales via hierarchical clustering (originating for instance from isothermal fluctuations in the density of the baryons, or as well from adiabatic fluctuations if the universe is dominated by cold, weakly interacting particles), the shapes of the collapsed objects, in the absence of significant rotation, are not expected to be very flat, because pressure balances gravity early in the collapse of each object. The first objects to collapse here have masses only slightly above the Jeans mass (Peebles and Dicke 1968; Peebles 1983), and while the clustering proceeds to larger scales, the Jeans mass grows accordingly as gravity builds up dispersion velocities. The superclusters in the I scenario have not collapsed yet, and their shapes should therefore not deviate much from the shapes in the initial distribution. In the competing scenario (hereafter the A scenario), where superclusters originate from a truncated spectrum of fluctuations with an excess of power on large scales (e.g., adiabatic fluctuations of baryons or massive neutrinos), the shapes are expected to be rather *flat* or *elongated* on large scales because pressure is negligible during the collapse of superclusters, i.e., the Jeans mass is many orders of magnitude smaller. Primordial, anisotropic, streaming velocities, which are coherent on the scale of the collapsing superclusters, induce very aspherical collapses that end up in thin "pancakes" or "cigars" (Zel'dovich 1970).

[1] Department of Astronomy, Yale University.
[2] Department of Astronomy, University of California, Berkeley.
[3] Institute of Astronomy, Cambridge, England.

As a part of the ongoing effort to distinguish between the theoretical scenarios when confronted with observations, we find it crucial to quantify, and be able to measure objectively, this property of flattening of the large-scale distribution of galaxies. The two-point correlation function, when analyzed directly in three dimensions from deep redshift surveys (e.g., Davis and Peebles 1983; Einasto *et al.* 1983), is found to provide a marginally sensitive test for the desired property (see Dekel and Aarseth 1984) in favor of the A scenario, but is clearly not the ideal statistics for that purpose because it measures shapes only indirectly, through their effects on other properties of clustering. Other attempts have been made to measure filamentary structure in two-dimensional data (Fesenko 1982; Doroshkevich *et al.* 1983; Kuhn and Uson 1982; Moody, Turner, and Gott 1983; J. A. Tyson, private communication), but with limited success so far in distinguishing between the major scenarios. The Soviet group (Zel'dovich, Einasto, and Shandarin 1982; Einasto *et al.* 1983) has proposed a test based on percolation theory and applied it to three-dimensional numerical models in comparison with the Center for Astrophysics (CfA) redshift sample. We find (§ III and Dekel and West 1984) that the maximum percolation length is not always useful in distinguishing between more realistic numerical simulations of the major scenarios. Furthermore, a major difficulty for any of the three-dimensional tests arises from the fact that observed redshift samples are not so easily converted to three-dimensional spatial distributions of galaxies because of the large dispersion velocities in rich clusters.

In the process of looking for a general statistical test for this purpose, we report here on a very simple test that makes use of rich clusters of galaxies to probe elongation of structures on larger scales and which has been found to be successful. Clusters are known to accumulate in superclusters (see Bahcall and Soneira 1984) and to show well-defined position angles (major axes) (see Carter and Metcalfe 1980; Binggeli 1982).

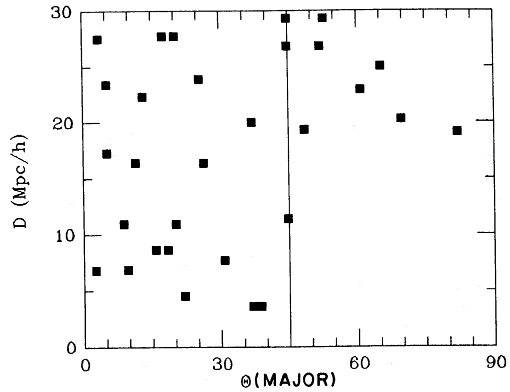


FIG. 1.—Binggeli's effect. The parameter $\theta$ is the angle between the major axis of an Abell cluster and the line connecting its center of mass to that of its nearest neighboring cluster, and $D$ is the spatial distance between the clusters (from Binggeli 1982).

At least in two major superclusters, Coma and Perseus, the cluster position angles are known to be aligned with the supercluster major axes (Oort 1983, and references therein). Binggeli (1982) has given more significance to this effect by finding that clusters of galaxies in general "tend to point toward each other." For each of the 44 Abell clusters he studied, Binggeli has determined the position angle of the major axis, using the 50 brightest members of the cluster, and the position angles of the lines connecting its center of mass to the centers of mass of neighboring clusters. In Figure 1 we show Binggeli's results for nearest neighboring clusters, where $\theta$ is the angle between the position angles described above, and $D$ is the three-dimensional separation of the clusters, obtained using their redshifts. There is a striking alignment of the orientations on scales below 20 Mpc $h^{-1}$ which extends out to 50 Mpc $h^{-1}$. Unlike many other cases in this field, there is no need here for any fancy statistics to see the effect, and it has been demonstrated by Binggeli, using Monte-Carlo techniques, that the errors made in determining $\theta$ are indeed very small.

The possible interpretation of Binggeli's (1982) alignments is apparently ambiguous: while such an effect may be a natural consequence of the large-scale *flattening* in the A scenario, where anisotropic shapes and velocity dispersions in the clusters have been induced by the anisotropic collapse of the parent supercluster (see Oort 1983), it may alternatively be a result of *tidal* interactions between protoclusters which act in the I scenario as well (as has been recognized by Binggeli himself). This assertion is based on the estimates (Binney and Silk 1979; Palmer 1983) that mutual tides in the protocluster stage are indeed capable of inducing prolate shapes that point to each other.

In order to identify the actual source of the alignment, we have applied an analysis similar to Binggeli's (1982) to the clusters we identify in $N$-body simulations of different cosmological scenarios. The results give an unambiguous answer: a very similar alignment shows up in the A scenario, while it is completely absent in the I scenario. It seems that tidal interactions do not do the job, perhaps because of the presence of underdense regions near, or around, the clusters. It means that the observed alignment provides evidence in favor of the A scenario.

In § II we describe the cosmological simulations and the proposed test and show the results. In § III we apply some other tests to the simulated samples, and in § IV we discuss our results and their cosmological implications.

## II. ALIGNMENT OF CLUSTERS

### *a*) *Simulations*

The simulations used here are based on a comoving version of an $N$-body code (Aarseth 1984) which integrates directly the Newtonian equations of motion of the particles, with a chosen softening of the potential on small scales. To simulate the I scenario we use the 4000 body simulation of Aarseth, Gott, and Turner (1979, hereafter AGT) and three realizations of similar 1000 body simulations by Frenk, White, and Davis (1983, hereafter FWD, the I simulations referred to as FWDI), both in an Einstein–de Sitter universe ($\Omega = 1$) and starting with a white-noise spectrum ($n = 0$). For the A scenario, we use two recent 10,000 body simulations (with $\Omega = 1$) from a series of simulations by Dekel and Aarseth (1984, hereafter DA) and a set of five 1000 body simulations, four of which are by FWD (their models A) and the fifth is by DA (model SG) (all five models are referred to hereafter as FWDA). These simulations started with an adiabatic spectrum that is a white noise on large scales and is truncated below a critical damping length scale, $\lambda_D$. In one case there is an additional component of scale-free white noise (isothermal fluctuations?) that dominates on small scales. The particles were first distributed uniformly inside a unit sphere, at the points of a cubic grid (model ADG with $N \approx 10{,}500$ and FWDA) or, alternatively, at random (model ADR with $N \approx 8000$). (Models ADG and ADR are models G and R of DA.) Then, the position and the velocity of each particle were perturbed by a superposition of 1000, small-amplitude plane waves, assuming random phases and wave-numbers, $k$, that were chosen at random in the phase-space shell $k_{\min}^3 < k^3 < k_{\max}^3$, where $k_{\min} = 2\pi$ and $k_{\max} = 3.33\pi$ (except for ADR where $k_{\max} = 5\pi$). This corresponds to superclusters with diameters $\lambda = 2\pi/k$ between $\lambda_D = 0.6$ (0.4 for ADR and $\lambda = 1$. The evolution of each system has been followed in the very linear regime by the approximation of Zel'dovich (1970), until a stage where the rms density contrast was $\sim 0.25$. Then, the cosmological expansion factor was set to $a = 1$ and the $N$-body simulation started. The first pancakes reached singularities at a time stage corresponding to $a \approx 4$. These dynamical simulations are also compared to a Poissonian sample of 4000 bodies whose positions were randomly distributed in a unit sphere.

The distribution of galaxies in models AGT, ADR, and ADG at the times that correspond to the present epoch are shown in Figure 2 (*upper*) as viewed from one direction. A cell-like structure of filaments on the scale of $\lambda_D$ can be recognized by the eye in ADG and ADR and is absent in AGT. It is less pronounced in ADR because, first, each line of sight crosses approximately five cells of superclusters and voids, second, the resolution is lower inside each supercluster, and third, they are broken into rich clusters. Even the clear distinction between ADG and AGT is less pronounced when the systems are viewed from other directions, and, as mentioned before, it is not easy to quantify.

The stages of the simulations that correspond to the

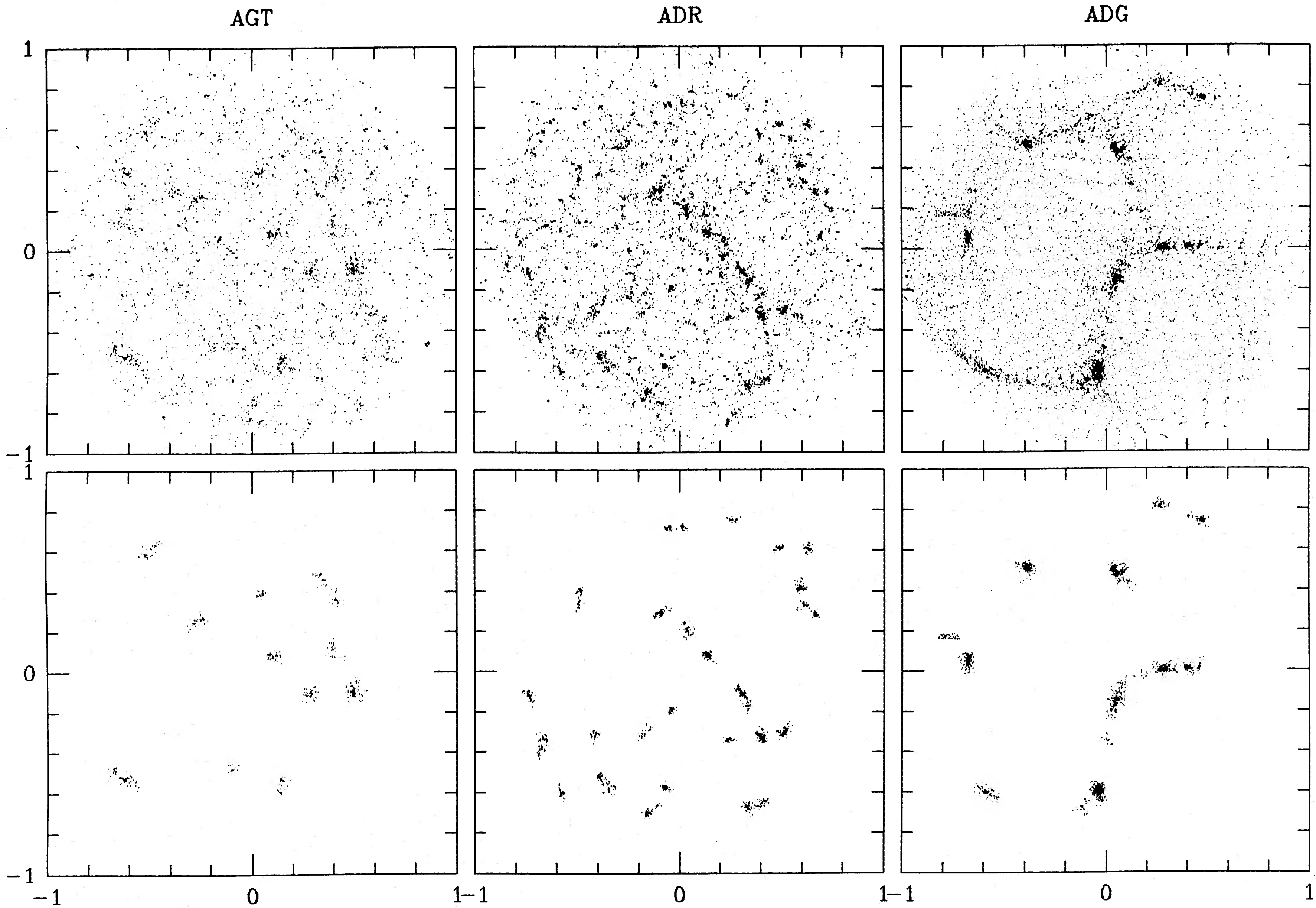


FIG. 2.—Projections of models ADG and ADR of the A scenario and AGT of the I scenario. The diameter of the sphere corresponds to 100 Mpc $h^{-1}$ (150 Mpc $h^{-1}$ in ADR) and the minimal wavelength to 30 Mpc $h^{-1}$. (*upper*) All particles representing the distribution of galaxies. (*lower*) The rich clusters identified with $d$ as given in Table 1.

TABLE 1

CLUSTER ALIGNMENTS

| Model | $N$ | $d/d_0$ | $N_{min}$ | $D$ (Mpc $h^{-1}$) | $\langle \cos \theta \rangle$ 3-D Minor Axis | $\langle \cos \theta \rangle$ 3-D Interm. Axis | $\langle \cos \theta \rangle$ 3-D Major Axis | $\langle \theta \rangle$ 2-D Major Axis (degrees) |
|---|---|---|---|---|---|---|---|---|
| ADG | 10439 | 0.31 | 35 | <30 | $0.304 \pm 0.055$ | $0.285 \pm 0.055$ | $0.798 \pm 0.054$ | $25.3 \pm 3.0$ |
| | | | | >30 | $0.563 \pm 0.025$ | $0.471 \pm 0.025$ | $0.456 \pm 0.025$ | $47.6 \pm 1.3$ |
| ADR | 7864 | 0.31 | 30 | <30 | $0.339 \pm 0.039$ | $0.484 \pm 0.043$ | $0.599 \pm 0.043$ | $35.7 \pm 2.1$ |
| | | | | >30 | $0.482 \pm 0.021$ | $0.487 \pm 0.022$ | $0.521 \pm 0.020$ | $42.9 \pm 1.1$ |
| AGT | 4000 | 0.30 | 20 | <30 | $0.434 \pm 0.037$ | $0.575 \pm 0.042$ | $0.479 \pm 0.049$ | $43.8 \pm 2.2$ |
| | | | | >30 | $0.507 \pm 0.027$ | $0.456 \pm 0.025$ | $0.521 \pm 0.027$ | $44.4 \pm 1.4$ |
| Random | 4000 | 0.6 | 20 | <30 | $0.438 \pm 0.045$ | $0.555 \pm 0.045$ | $0.475 \pm 0.048$ | $44.0 \pm 2.1$ |
| | | | | >30 | $0.491 \pm 0.024$ | $0.504 \pm 0.023$ | $0.514 \pm 0.022$ | $44.9 \pm 1.2$ |
| FWDA | 1000 × 5 | 0.31 | 7 | <30 | $0.315 \pm 0.033$ | $0.400 \pm 0.037$ | $0.744 \pm 0.031$ | $29.8 \pm 1.7$ |
| | | | | >30 | $0.540 \pm 0.018$ | $0.495 \pm 0.019$ | $0.475 \pm 0.018$ | $47.0 \pm 1.0$ |
| FWDI | 1000 × 3 | 0.12 | 7 | <30 | $0.435 \pm 0.026$ | $0.520 \pm 0.029$ | $0.537 \pm 0.026$ | $43.8 \pm 1.4$ |
| | | | | >30 | $0.538 \pm 0.018$ | $0.478 \pm 0.015$ | $0.483 \pm 0.014$ | $47.5 \pm 0.7$ |
| ADG (Cluster-Cluster) | | | | <30 | $0.666 \pm 0.069$ | $0.633 \pm 0.072$ | $0.678 \pm 0.053$ | $34.6 \pm 2.8$ |
| | | | | >30 | $0.469 \pm 0.025$ | $0.523 \pm 0.026$ | $0.504 \pm 0.023$ | $46.8 \pm 1.2$ |
| Binggeli (All) | | | | <25 | ... | ... | ... | $36 \pm 5$ |
| | | | | $25 < D < 50$ | ... | ... | ... | $41 \pm 2$ |
| Binggeli (Nearest) | | | | <15 | ... | ... | ... | $23.0 \pm 4.1$ |
| | | | | <30 | ... | ... | ... | $29.5 \pm 4.4$ |

present epoch are determined by the two-point correlation function (DA). In the A simulations, its slope grows in time and fits the shape of the observed one only at one given stage of the evolution which corresponds to $a \approx 5$–6. The observed clustering length of galaxies (at which the correlation function is unity) $r_0 \approx 5$ Mpc $h^{-1}$ (cf. Davis and Peebles 1983), then corresponds to $r_0 \approx 0.1$ (0.67 in ADR) in the units of the simulations (with $G = 1$, $m = 1$). With this scaling, the diameter of the system corresponds to 100 Mpc $h^{-1}$ (150 in ADR) and the diameters of pancakes correspond to 30 Mpc $h^{-1}$. The mass within a sphere of diameter $\lambda_D$ is $M_D = 3.6 \times 10^{15} M_\odot h^2$. In the I simulations, the correlation function evolves in a self-similar way, and we choose accordingly the stage at which $r_0 \approx 0.1$ to represent the present universe ($a \approx 6$–7). The visible differences in cluster richnesses between the models are not real. They mainly reflect the differences in the numbers of particles that were simulated.

### *b) Analysis of Cluster Orientations*

The procedure adopted here for identifying clusters in the simulations is the simple method of linking near neighbors, similar to that used by Einasto *et al.* (1983). For a given value of the separation parameter $d$, each particle is linked to every other particle whose distance from it is shorter than $d$. Particles that are linked to each other, either directly or via other particles ("friends of friends"), construct a cluster. The parameter $d$ determines the richness of the clusters identified and is closely related to the mean overdensity within the clusters relative to the mean background density. A value of $d$ just below the mean separation between nearest neighbors, $d_0$, gives one huge cluster of very low overdensity, while a much smaller $d$ picks up only clusters which are at the high-density peaks. The values of $d$ chosen to identify rich clusters in the present context (Table 1) correspond to an overdensity greater than $\sim 35$. A requirement of a minimum number of members, $N_{min}$, was imposed (Table 1) in order to focus on the richest clusters that would resemble the Abell clusters as much as possible. Following the above procedure, we find in each simulation typically 10 such clusters ($\sim 30$ in ADR) which contain $\sim 10\%$ of the total mass, $\sim 10^{15} M_\odot$ each. The clusters identified in ADG, ADR, and AGT, are shown in Figure 2 (*lower*), projected as above.

The following procedure has been repeated using a more elaborate overdensity criterion for identifying clusters. The clusters identified by overdensity were found to be slightly less flattened, but there was no apparent effect on the final alignments detected. It is because the determination of the directions of the principal axes of the clusters is very insensitive to the way in which the clusters are identified which makes this test so simple and unambiguous.

Once a cluster has been identified, its principal axes of inertia were computed from the distribution of galaxies within it, by solving the corresponding eigenvalue equation. The principal axes were computed in three dimensions and also in three orthogonal, two-dimensional projections. All clusters are flat enough for their principal axes to be determined uniquely (we discuss the actual axial ratios in § III). The angle $\theta$ is the angle between a principal axis of a cluster (in three-dimensions or in two-dimensional projections alternatively) and the line connecting its center of mass to that of another cluster. $D$ is the three-dimensional distance between the centers of mass.

A correlation between the orientations on very large scales ($D > 1$) can arise from edge effects, which tend to bias the orientations of clusters near the edges of the system. We therefore exclude clusters whose centers of mass are closer than 0.1 to the nearest edge.

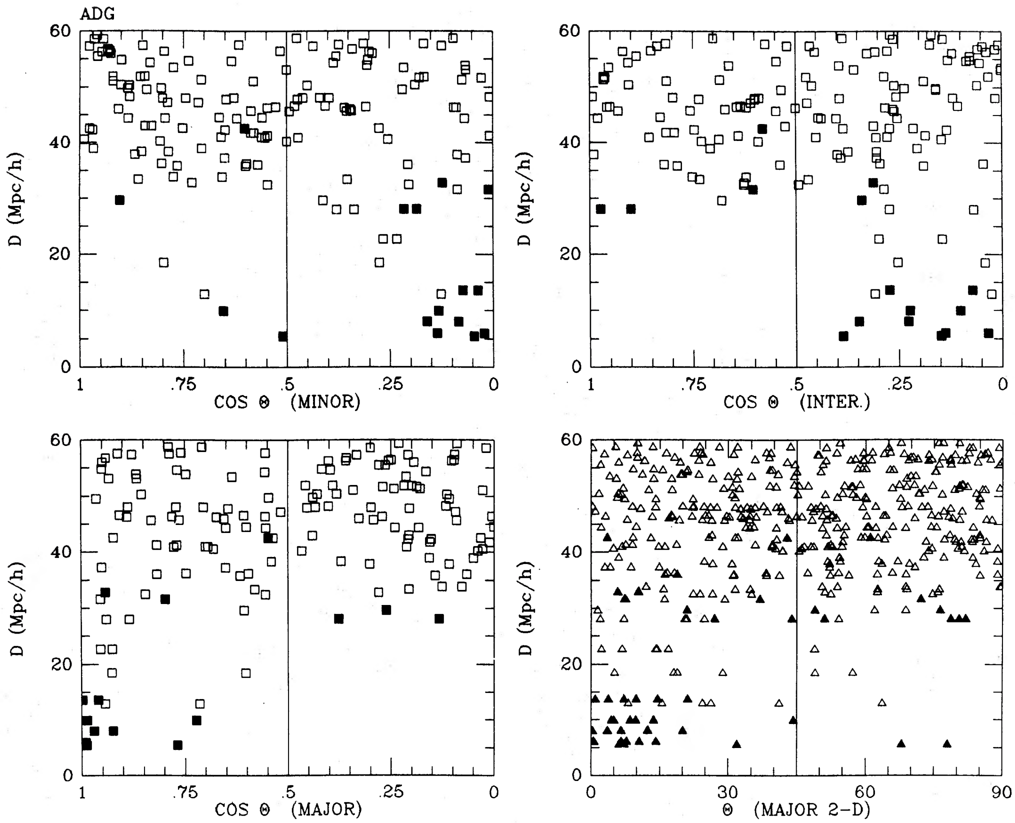


FIG. 3*a*

FIG. 3.—Alignments in the simulations. The parameter $\theta$ is the angle between a principal axis of a cluster and a line connecting its center of mass to that of another cluster, and $D$ is the spatial distance between the clusters. $D = 30$ Mpc $h^{-1}$ corresponds to $D = 0.6$ in the units of the experiment ($D = 0.4$ in ADR). Filled symbols correspond to nearest clusters. (*a*) Model ADG, (*b*) model ADR, (*c*) model AGT, (*d*) a random distribution, (*e*) five A models FWDA, (*f*) three I models FWDI, (*g*) model ADG: here $\theta$ is the angle between the principal axes of every two clusters.

### *c*) *Results*

The results are shown in Figure 3 and in Table 1. Figures 3*a*–3*d* correspond to the large-*N* models ADG, ADR, AGT, and the "random" case respectively. Figures 3*e* and 3*f* are superpositions of the 1000 body FWDA and FWDI models respectively. In the former, the large number of particles in each cluster makes the determination of the principal axes and the centers of mass be very precise, and in the latter the large total number of clusters improves the statistical significance of the measurement of alignments. Each part of the figure consists of four plots describing the alignments of the three-dimensional minor, intermediate, and major axes and the two-dimensional major axes respectively. $D$, translated to Mpc $h^{-1}$, is plotted against cos $\theta$ (which is expected to be distributed uniformly between 0 and 1 in a random three-dimensional distribution) or against $\theta$ (which is expected to be distributed uniformly between 0° and 90° in a two-dimensional random distribution). Filled symbols correspond to the nearest neighbor of each cluster, and open symbols correspond to all other neighbors. Figure 3*g* shows for comparison in model ADG the alignments of every two clusters relative to each other (instead of the alignments of each cluster with the line connecting their centers). In Table 1 the data have been divided into two bins corresponding to $0 < D < 30$ Mpc $h^{-1}$ and $30 < D < 60$ Mpc $h^{-1}$, respectively, and in each bin the mean value of cos $\theta$ (or $\theta$) has been calculated together with its standard deviation. Binggeli's (1982) data have been analyzed similarly, and the means are given in the table.

It is evident from the plots that an effect similar to the observed one is *present* in the A scenario and is *absent* in the I scenario. The results from the I models AGT and FWDI resemble the results from the random distribution within 1 $\sigma$. In the A simulations, for $D < 30$ Mpc $h^{-1}$, the minor axes tend to be perpendicular to the lines connecting the clusters, where $\langle \cos \theta \rangle$ deviates from 0.5 by 3.6 $\sigma$, 4 $\sigma$, and 5.6 $\sigma$ for ADG, ADR, and FWDA respectively. This indicates that the superclusters are indeed flattened at least along one direction, but it does not distinguish between oblate and prolate configurations (pancakes and cigars). The major axes tend to be parallel to the connecting lines, where $\langle \cos \theta \rangle$ deviates from 0.5 by 5.5 $\sigma$, 2.3 $\sigma$, and 7.9 $\sigma$ respectively. This indicates that, at this stage, the systems tend to be cigars more than pancakes—a tendency which is weaker in ADR. The intermediate axes support this interpretation: they are strongly misaligned with the lines connecting the clusters in ADG and in FWDA, similarly to the minor axis, indicating cigars. In ADR there is no such misalignment, indicating pancakes.

The projected distribution resembles the observed data,

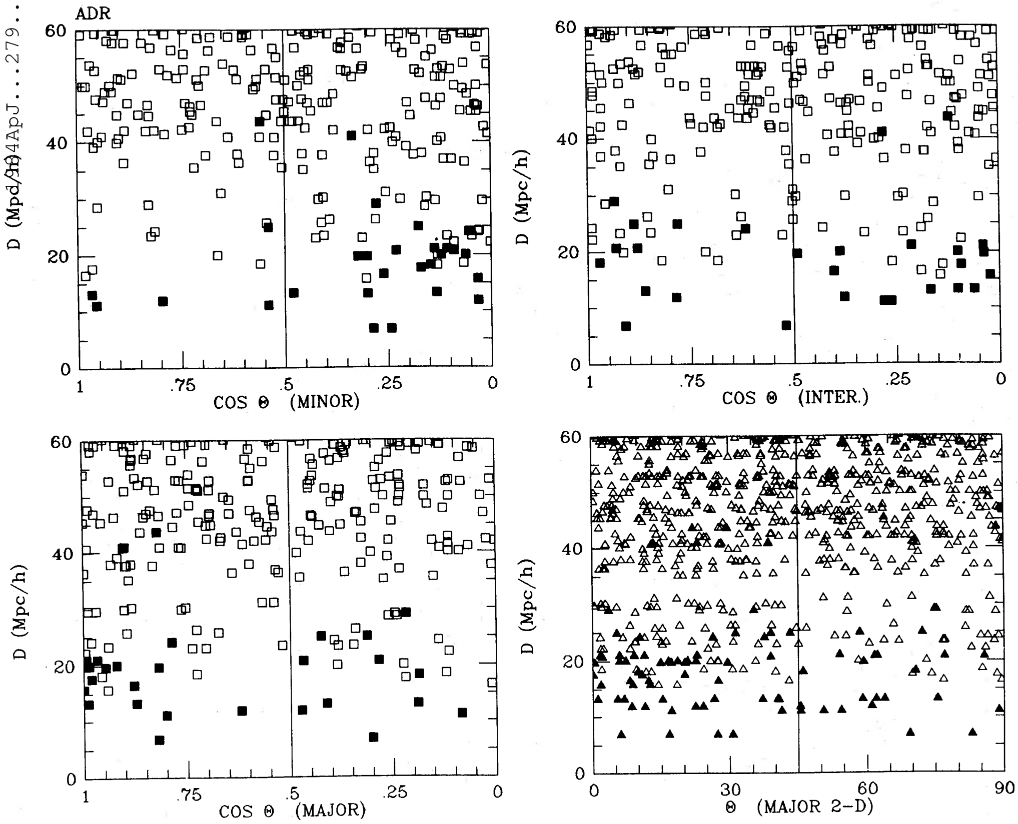
ADR
60
40
20
0
D (Mpc/h)
1
.75
.5
.25
0
COS Θ (MINOR)
COS Θ (INTER.)
COS Θ (MAJOR)
30
60
90
Θ (MAJOR 2-D)

FIG. 3*b*

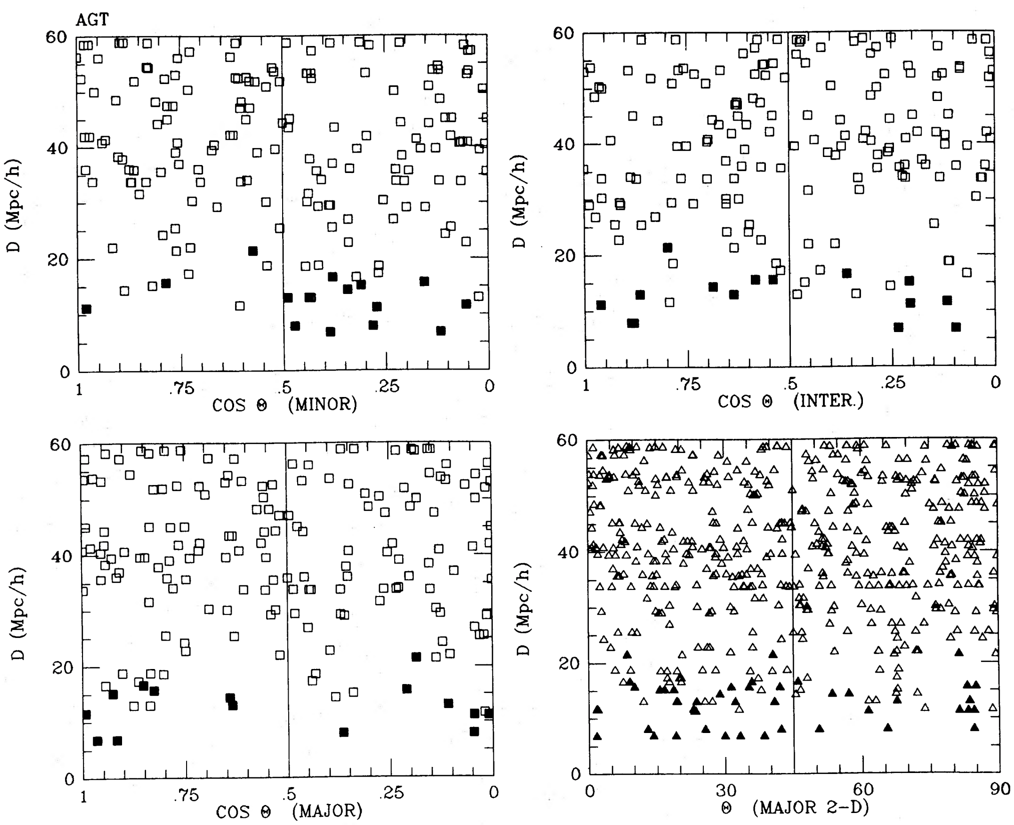
AGT
60
40
20
0
D (Mpc/h)
1
.75
.5
.25
0
COS Θ (MINOR)
COS Θ (INTER.)
COS Θ (MAJOR)
30
60
90
Θ (MAJOR 2-D)

FIG. 3*c*

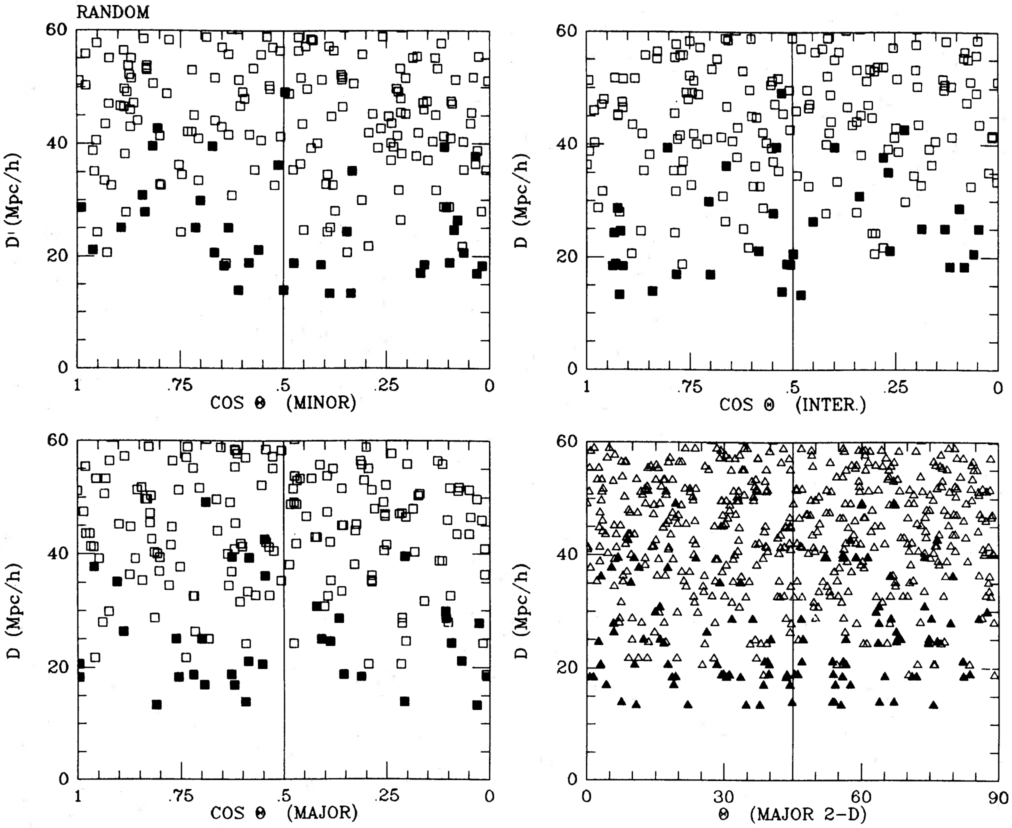
RANDOM
D' (Mpc/h)
COS Θ (MINOR)
D (Mpc/h)
COS Θ (INTER.)
D (Mpc/h)
COS Θ (MAJOR)
D (Mpc/h)
Θ (MAJOR 2-D)

FIG. 3*d*

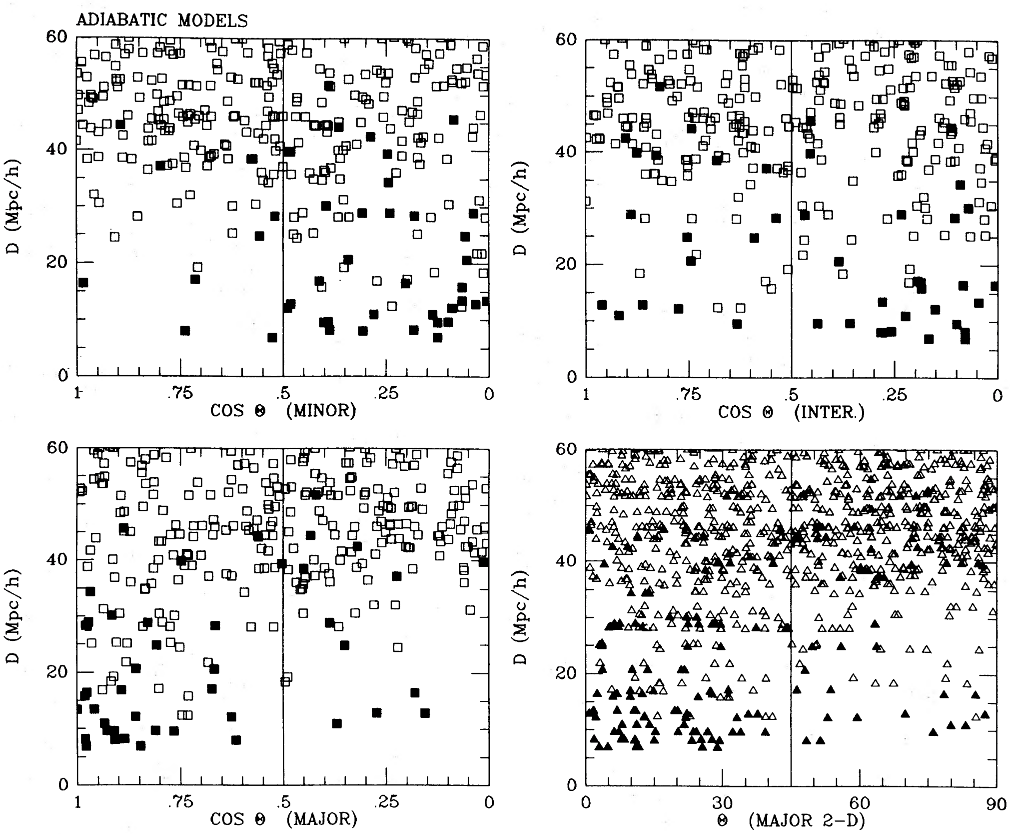
ADIABATIC MODELS
D (Mpc/h)
COS Θ (MINOR)
D (Mpc/h)
COS Θ (INTER.)
D (Mpc/h)
COS Θ (MAJOR)
D (Mpc/h)
Θ (MAJOR 2-D)

FIG. 3*e*

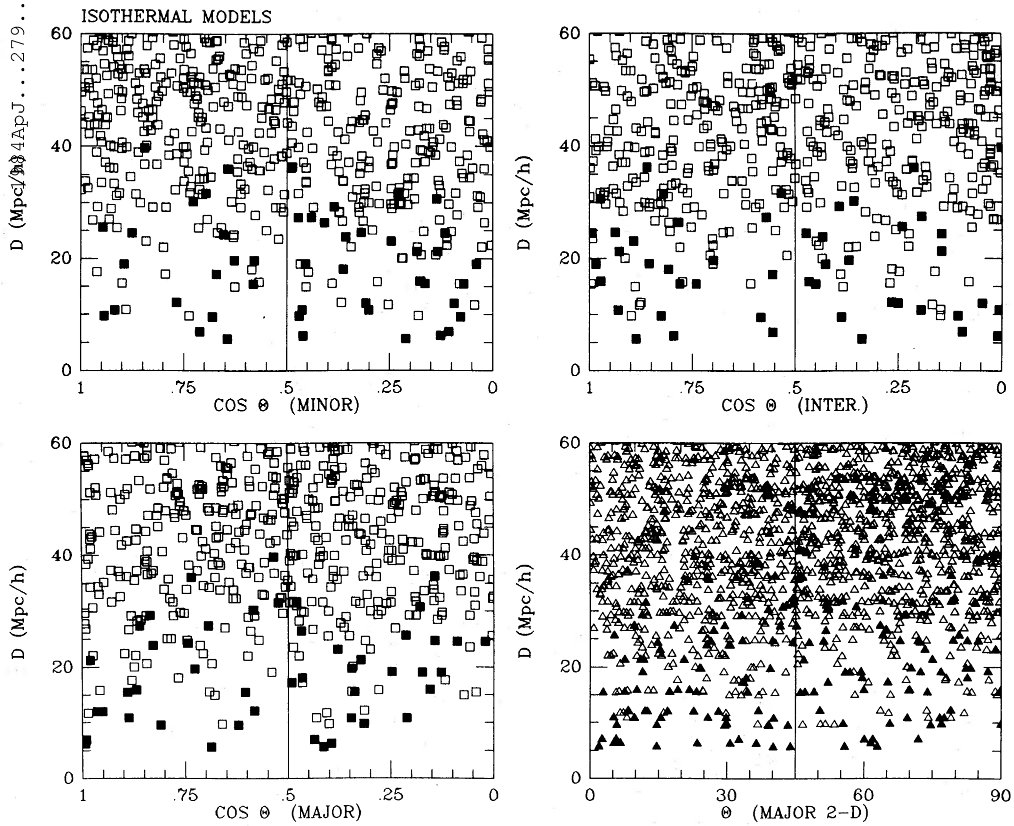

ISOTHERMAL MODELS
D (Mpc/h)
COS Θ (MINOR)
COS Θ (INTER.)
COS Θ (MAJOR)
Θ (MAJOR 2-D)


FIG. 3*f*

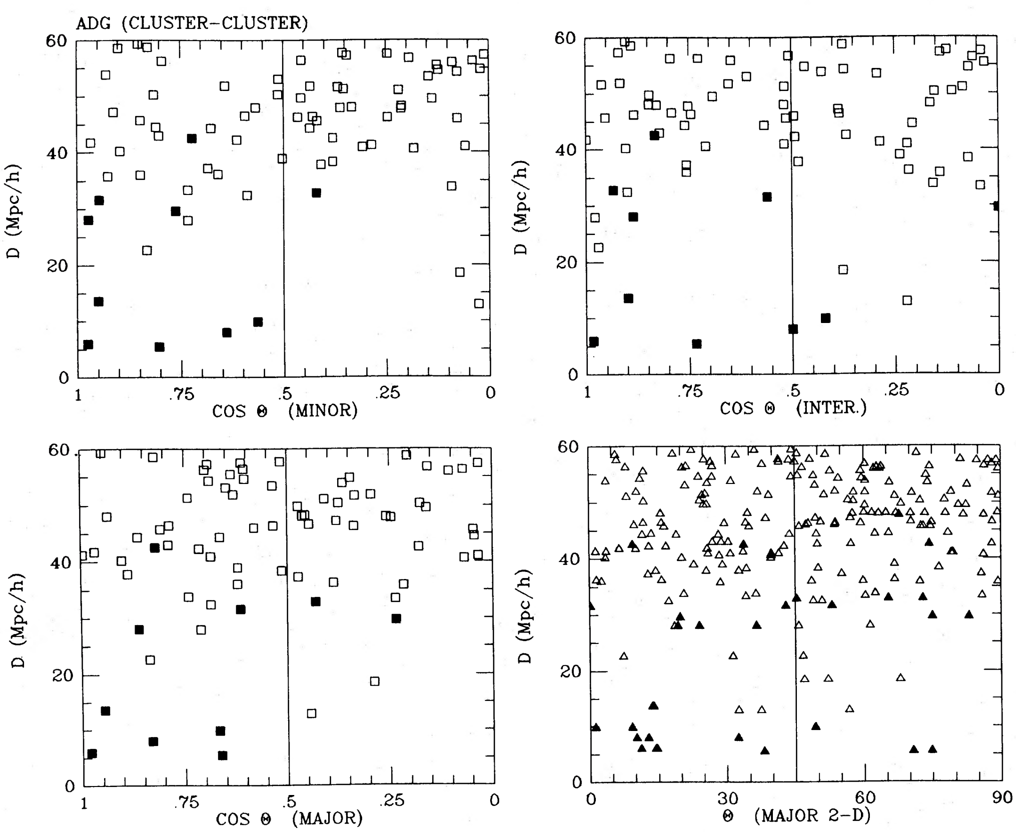

ADG (CLUSTER-CLUSTER)
D (Mpc/h)
COS Θ (MINOR)
COS Θ (INTER.)
COS Θ (MAJOR)
Θ (MAJOR 2-D)


FIG. 3*g*

where on small scales $\langle \theta \rangle$ is 6.6 $\sigma$ and 5.4 $\sigma$ away from 45° in ADG, and in the observations when only nearest neighboring clusters are taken into account. In ADR $\langle \theta \rangle$ is similar to that obtained by Binggeli (1982) taking into account all clusters, where it is 4.4 $\sigma$ and 1.8 $\sigma$ away from 45° respectively.

The effect is somewhat weaker in ADR relative to the other A models because the clusters develop there from the white noise on small scales before the large-scale adiabatic perturbations managed to collapse a substantial fraction of their way to pancakes. In all the A models, the alignment becomes much weaker on large scales, and in some cases even an anti-alignment shows up (presumably as a result of the edge effect mentioned above).

## III. SOME RELATED TESTS

We have applied two other tests to some of the simulated samples in order to gain some more insight into the actual shapes of the superclusters: an axial ratios test and the percolation test. The former was found to be qualitatively successful while the latter failed here. Nevertheless, we describe both here, especially because of the recent popularity of the percolation test. Eventually, we end up demonstrating how simple and sensitive the alignments test is in contrast to the other two.

The tests were applied to the following simulated samples with 1000 bodies: to a random Poissonian distribution, to 1000 particles chosen at random from the dynamical I simulation of AGT, to dynamical A simulations analogous to ADG and ADR, and in addition to a kinematical A simulation, ADZ, which started exactly as the analog to ADR, but where gravity has been completely suppressed on small scales and the trajectories of the particles have been computed using the linear approximation of Zel'dovich (1970).

### *a*) *Axial Ratios on Various Scales*

A direct measurement of the property that may distinguish between the scenarios may be the axial ratios of the clusters (superclusters) on the various scales. For varying values of $d$, we have repeated the procedure described in § II, but focused here on the ratio of the eigenvalues, i.e., the rms dimensions of the clusters along their principal axes. In Figure 4 we plot the axial ratios of the largest cluster as a function of $d$ for (*a*) the major and the minor axes and (*b*) the major and the intermediate axes. From Figure 6 below, the maximum supercluster size of $L_{\max} = 1$ corresponds to $d = 0.12$, and, indeed, the flattening becomes more pronounced below this scale in ADG and in ADR relative to AGT. Maximum flattening is achieved near $d = 0.08$, which corresponds to a length scale of $L_{\max} \approx 0.4$, just below the pancake scale ($\lambda_D = 0.6$). Recall that those three cases have similar correlation functions and can therefore be compared directly, while ADZ is less clustered on small scales, and the random distribution (Poisson) has zero correlation function on all scales.

Figure 4 can also distinguish between pancakes and cigars. In the dynamical simulations, ADG and ADR, the largest structure is cigar-like with axial ratios at $d = 0.08$ of 7:1.7:1 and 6:1.3:1, respectively, in agreement with the findings of § II. ADZ shows pancakes on slightly smaller scales, with axial ratios of 3.3:2.2:1 at $d = 0.06$.

There are several weaknesses to this kind of test. First, unlike the alignment test discussed in § II, the actual values obtained for the axial ratios are sensitive to the methods used to identify the clusters, to define the axial ratios, and to measure them. Second, the axial ratios depend on the number of particles in the cluster. Using samples that have the same number of particles within the clustering radius, $r_0$, gives clusters of comparable richnesses in the different cases (see Fig. 5), which can serve us as a first approximation, but the numbers are not identical and the differences have a significant effect on the axial ratios measured on small scales. Third, there is a noticeable flattening in the superclusters of the random distribution, which we find not trivial to take onto account when judging the significance of the flattening in the tested, clustered samples. Because of the above difficulties, we chose to limit the discussion to the largest cluster instead of averaging over several.

It is clear, though, that the axial ratio test is capable

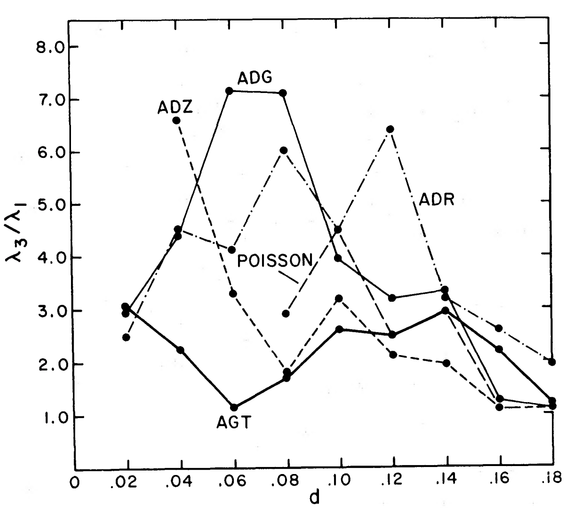


FIG. 4*a*

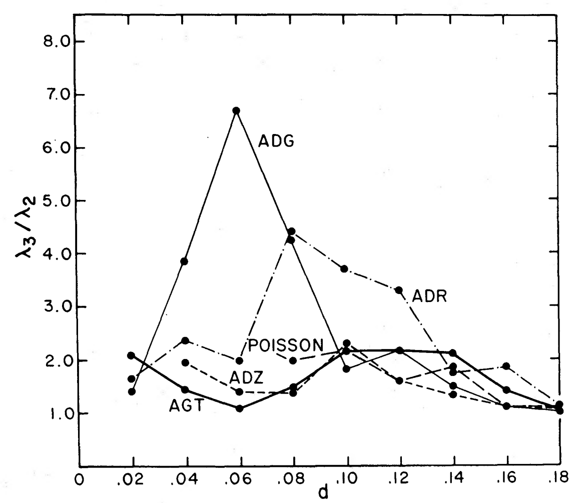


FIG. 4*b*

FIG. 4.—Axial ratios of the largest cluster as a function of scale via the separation parameter $d$. (*a*) Major/minor axes, (*b*) major/intermediate axes.

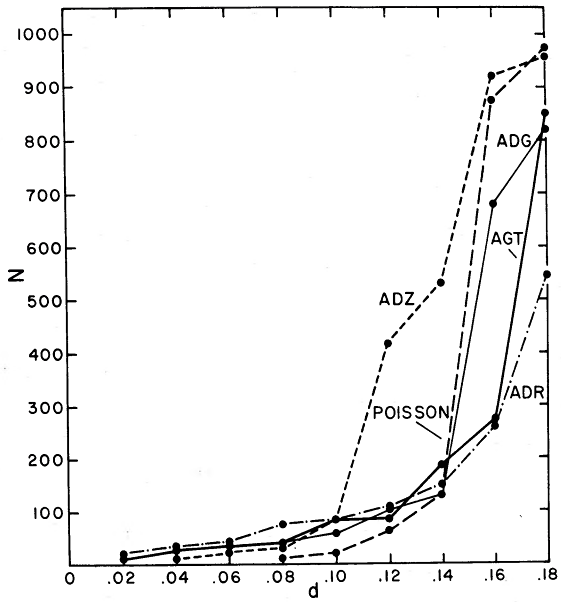


FIG. 5

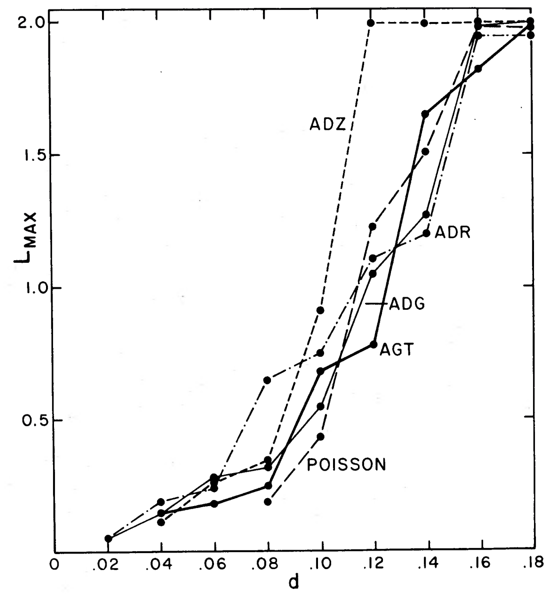


FIG. 6

FIG. 5.—The number of particles in the richest cluster as a function of the separation parameter $d$

FIG. 6.—Maximum percolation length as a function of the separation parameter $d$ in the simulations: $d = 0.1$ corresponds to 5 Mpc $h^{-1}$. The initial mean separation between nearest particles is 0.16.

of picking up the excess flattening of superclusters in the A scenarios relative to the I scenario, and can make, at least, a qualitative test. The axial ratios measured in the CfA sample by Einasto *et al.* (1983, Fig. 14) in a somewhat different manner shows indeed an excess of flattening in the range corresponding to $0.06 \leq d \leq 0.12$, in agreement with the A scenarios. We are in the process of generalizing this test and applying it to further observational data.

One simple, straightforward generalization of this test has failed to distinguish between the scenarios. Instead of focusing on individual clusters, we considered the flattening of the distribution of particles in a neighborhood of a given size around every particle. For a given length scale $R$, we have computed for each particle the principal axes of the distribution of particles inside a sphere of radius $R$ around it, and compared the eigenvalues with the ones obtained in a random distribution of the same number of particles in a sphere of the same size. We then computed the averages of the largest eigenvalue and of the smallest one over all the particles as centers, their ratio indicating the degree of flattening in the whole sample. The test gave a clear signal of flattening in the A scenarios, but unfortunately it gave a similar signal in AGT too. The cause of this problem is the presence of rich clusters, each pair of them defining a preferred line, and each triplet defining a preferred plane. Since each supercluster has at the most a few rich clusters in it, those artificial lines and planes dominate and give a false signal. We are trying ways to improve this test, but we do not have great hopes here.

### *b) Maximum Percolation Length*

We have applied the percolation test suggested by Zel'dovich *et al.* (1982) to the same simulated samples. The procedure is very simple: for progressive values of the separation parameter $d$, we compute the corresponding values of $L_{max}$, the longest separation between any two galaxies that belong to the same cluster. $L_{max}$ is plotted against $d$ in Figure 6. Models ADG, ADR, and AGT are practically indistinguishable on all scales! They all essentially resemble the random distribution (although the correlation function is very different). Our understanding of this effect is that small-scale clustering makes it easy to percolate along short distances and hard to "jump" from cluster to cluster, while large-scale pancaking seems to have a negligible effect in a situation where small-scale clustering is developed, especially when the mean separation between neighboring particles, $d_0$, is larger than the clustering length scale, $r_0$. Here $d_0 \approx 0.16$ for the corresponding Poissonian distribution, and $r_0 \approx 0.1$ in the dynamical cases. It is much easier to percolate in ADZ because there is indeed no small-scale clustering there, so that the distance between nearest neighbors does not vary much throughout the sample, and the large-scale pancaking makes the actual $d_0$ along the percolation path smaller than in the random distribution.

Einasto *et al.* (1983) found that the same test was useful in distinguishing between other models of the scenarios A and I. In order to compare to their Figure 11, we note that our separation parameters are related by $r = (4\pi/3)^{1/3}d$ and estimate that $L = 100$ Mpc corresponds to our $L_{max} = 1$. The curve for ADZ is similar to the curve plotted by Einasto *et al.* for the A simulations of Klypin and Shandarin (1983). This partly reflects the suppression of gravity on small scales in their simulations, as a result of the cloud-in-a-cell method they have used (integrated by a fast Fourier transform technique), where the grid cell size was comparable to $r_0$. In our dynamical A simulations, the pancakes break into clusters, which make the pancakes harder to percolate through. Another cause for the difference in our results for the A simulations is the (sometimes ignored) dependence of the percolation test on the mean number density, $n$. The critical separation $d_c$, for which $L_{\max}$ reaches a certain value $L_c$, is expected to be related to the actual mean separation between neighboring particles along the percolation path, $d_0$. In the case of three-dimensional structures (e.g., Poissonian, $I$) $d_0 \propto n^{-1/3}$; but when the structures are very flattened, $d_0 \propto n^{-1/2}$ (for thin pancakes) or even $d_0 \propto n^{-1}$ (for thin cigars), so that it cannot be estimated *a priori* for the general A scenario. Hence, the $n$-dependence of $d_c$ is different in A versus I, which requires that tested samples must have the same densities. The difference between the percolation properties of the two scenarios is more pronounced when denser samples are compared. The samples used by Einasto *et al.* are indeed 4–8 times denser than our 1000 body samples used to test percolation here.

For the I scenario, Einasto *et al.* (1983) have used the static, hierarchical model of Soneira and Peebles (1978), which is built to have the proper 2–4 point correlation functions, and they found it to be very hard to percolate through. Note, however, that the hierarchical model makes a poor fit to the observed universe, e.g., when tested by Mead's statistics (Shanks 1979), and is perhaps not very realistic. We find it much easier to percolate in a more realistic dynamical model that simulates the I scenario. A further disturbing fact for the percolation test is that a non-clustered Poissonian distribution shows percolation properties similar to those of the clustered samples. We conclude that our limited experience with the percolation test raises some suspicion concerning its sensitivity as a general cosmological test. We study and discuss it in detail elsewhere (Dekel and West 1984).

## IV. DISCUSSION

We have found that the alignments of clusters of galaxies detected by Binggeli (1982) provide a useful test for distinguishing between the major competing scenarios for the formation of large-scale structure in the universe. The test is simple to apply both to observations and to numerical models because the position angle of a rich cluster is well defined in most cases and the procedure of finding it does not involve any large errors. The test was found to provide unambiguous results: the alignment is due to large-scale flattening of superclusters and is not produced by tidal interactions in the absence of large-scale flattening.

We do not attempt here to dig much further into the details of the tidal interactions between the protoclusters because the numerical simulations give the net result clearly enough for our purpose here. We believe that the analytical calculations by Binney and Silk (1979) and by Palmer (1983) overestimate the effect because they assume for the protoclusters overdense perturbations above a *uniform* background. When realistic protoclusters start contracting relative to the expanding background, however, they are likely to evacuate underdense regions around them, which tend to weaken their gravitational influence on other protoclusters. This can be illustrated by the following two simple examples. In the case of a spherically symmetric cluster surrounded by an underdense shell, there is a radius inside which the mean density matches the mean universal density. Such a sphere would exert *no* gravitational force on its surroundings. When a flattened cluster forms first, it evacuates regions in the direction of its minor axis (axes). Such an underdense region exerts negative tides on a protocluster that is forming on its other side which tend to induce a collapse along the direction of the minor axis of the original cluster, producing an *anti-alignment*. The general case is more complex and requires a study of "holes" which we intend to do separately. It is evident though that underdense regions are present between the clusters in the I simulations (see Aarseth and Saslaw 1982), and that they tend in general to weaken the mutual tides between the protoclusters.

The alignment of clusters indicates not only that superclusters are elongated, but that they have been formed *before* the rich clusters in them. This requires that superclusters form by aspherical collapse from an excess of large-scale fluctuations.

Our basic conclusion here applies to a variety of cosmological scenarios: the favored A scenario can originate from any spectrum of large-scale fluctuations that is truncated at the pancake scale, i.e., it can be adiabatic fluctuations that are either baryonic (Zel'dovich 1970), or dominated by $\sim 30$ eV neutrinos (see Doroshkevich *et al.* 1981, and references therein), or even an excess of isothermal fluctuations if baryons roughly close the universe (Hogan and Kaiser 1983). The rejection of the so-called I scenario applies to any initial fluctuations that form structure solely along the route from small to large scales, such as purely isothermal fluctuations in the baryons' density (Peebles and Dicke 1968), or adiabatic fluctuations of $\geq 1$ keV, cold, weakly interacting "ions," or light axions (see Peebles 1982, 1983; Primack and Blumenthal 1983, and references therein). It is worth noting that just having some power on large scales is not enough: a spectrum that has a lot of power on large scales ($n < 0$, say) may produce elongated structures, but as long as structure still evolves from small to large, such that clusters form before superclusters, there is no apparent reason for them to be aligned. It seems that the spectrum must have had a real excess of power on scales above a critical scale that corresponds to pancakes.

Failures to detect such an alignment in *galaxies* relative to background clusters or superclusters (Adams, Strom, and Strom 1980; Gregory, Thompson, and Tifft 1981; MacGillavry *et al.* 1982; Helou and Salpeter 1982; Kapranidis and Sullivan 1983; Valdes, Tyson, and Jarvis 1983) indicate that a similar conclusion is *not* necessarily true for galaxies: they could have formed either as a result of the pancaking of superclusters, as suggested by the dissipative pancake theory of Zel'dovich (1970) or, as well, independently, from initial fluctuations on small scales, as suggested by the hybrid, nondissipative pancake scenario (cf. Dekel 1982, 1983*a*, *b*). The detected alignment of brightest cluster members with their parent clusters (see Carter and Metcalfe 1980; Binggeli 1982) is probably an evolutionary effect within the clusters. Another possible exception may be the tendency for alignment for galaxies in the Coma Cluster (Djorgovski 1983), but the fact that the alignment is exactly east-west there makes one worried about possible systematic errors in the data.

There is other evidence in support of a hybrid scenario, such as the failure of a pure, adiabatic spectrum of baryons (Dekel 1982; DA) or of massive neutrinos (White, Frenk, and Davis 1983) to reproduce the observed correlation function of galaxies, unless the pancakes have collapsed after $z \approx 1$ if $\Omega = 1$ (or after $z \approx 2$ if $\Omega_0 = 0.1$), so that galaxies have to be formed *before* superclusters. This is supported by the presence of galaxies away from pancakes and by the flattening of superclusters which again points to a similarly recent collapse (Dekel 1983*a*, *b*). If superclusters are indeed so young dynamically, then, according to the conclusions of this work, rich clusters must be young too. Hence, the hybrid scenario predicts that rich clusters should show dynamical evolution already at $z \sim 1$. This is in agreement with constraints obtained from the present overdensity in Abell clusters ($\delta\rho/\rho \approx 500$ inside the Abell radius of 1.5 Mpc $h^{-1}$ for richness $R = 1$) that also indicate $z < 1$ for their collapse ($\Omega = 1$).

Although the alignment of clusters is clear both in the observations and in the simulations, it would gain some more weight if the samples were enlarged. One may extend Binggeli's (1982) analysis of clusters for a larger sample or use brightest cluster members instead, based on their tight alignment with their parent clusters. In Binggeli's analysis of the latter, the effect seems to be weaker when only nearest neighbors are concerned, which makes one wish to see the test applied to other samples as well. We encourage a study similar to that of Binggeli for the possible alignment of smaller clusters and groups of galaxies, and even of pairs (see Tifft 1980).

We wish to emphasize that an alignment of each cluster with its parent supercluster should be easier to detect than a relative alignment of every two clusters, as can be seen by comparing Figures 3*a* and 3*g*. The former gives twice as many points in a $D$-$\theta$ diagram, and the tendency toward small (or large) angles in the case of elongated structures is relatively smeared out in the latter: when, for example, the principal axes of two clusters both form an angle $\theta$ with the line connecting their centers, the relative angle between their axes can be anywhere in the interval $(0, 2\theta)$. From the theoretical side, it would also be of interest to see how the test works in other types of cosmological scenarios.

The success of this simple test makes us optimistic about generalizing it to make a more general statistical test. The idea is to measure for any given scale the alignment of the configuration with respect to a larger scale. This work is currently in progress and already gives very promising results (West and Dekel 1984).

We gratefully thank Simon White, Carlos Frenk, and Marc Davis for allowing the use of their simulations and for helpful comments. We acknowledge a collaboration with Tsvi Piran on the axial ratios test. A. D. and M. J. W. thank Simon White, the Department of Astronomy, and the Space Sciences Laboratory of the University of California at Berkeley for their hospitality during the last stage of this work.

## REFERENCES


Aarseth, S. J. 1984, in *Methods of Computational Physics*, ed. J. U. Brackbill and B. I. Cohen (New York: Academic), p. 1.
Aarseth, S. J., Gott, J. R., III, and Turner, E. L. 1979, *Ap. J.*, **228**, 664 (AGT).
Aarseth, S. J., and Saslaw, W. C. 1982, *Ap. J.* (*Letters*), **258**, L7.
Adams, M. T., Strom, K. M., and Strom, S. E. 1980, *Ap. J.*, **238**, 445.
Bahcall, N., and Soneira, R. M. 1984, Princeton Observatory Preprint −049.
Binggeli, B. 1982, *Astr. Ap.*, **107**, 338.
Binney, J., and Silk, J. 1979, *M.N.R.A.S.*, **188**, 273.
Carter, D., and Metcalfe, N. 1980, *M.N.R.A.S.*, **191**, 325.
Davis, M., and Peebles, P. J. E. 1983, *Ap. J.*, **267**, 465.
Dekel, A. 1982, *Ap. J.* (*Letters*), **261**, L13.
———. 1983*a*, *Ap. J.*, **264**, 373.
———. 1983*b*, *IAU Symposium 102*, ed. G. Abell and G. Chincarini (Dordrecht: Reidel), p. 249.
Dekel, A., and Aarseth, S. J. 1984, *Ap. J.*, submitted.
Dekel, A., and West, M. J. 1984, Yale University preprint.
Djorgovski, S. 1983, *Ap. J.* (*Letters*), **274**, L7.
Doroshkevich, A. G., Khlopov, M. Yu., Sunyaev, R. A., Szalay, A. S., and Zel'dovich, Ya. B. 1981, in *Proceedings of the Tenth Texas Symposium*, ed. R. Ramaty and F. C. Jones, *Ann. NY Acad. Sci.*, **375**, 32.
Doroshkevich, A. G., Kotok, E. V., Shandarin, S. F., and Sigov, Yu. S. 1983, *M.N.R.A.S.*, **202**, 537.
Einasto, J., Klypin, A. A., Saar, E., and Shandarin, S. F. 1983, preprint.
Fesenko, B. I. 1982, *Soviet Astr. Letters*, **8**, 247.
Frenk, C. S., White, S. D. M., and Davis, M. 1983, *Ap. J.*, **271**, 417 (FWD).
Gregory, S. A., Thompson, L. A., and Tifft, W. G. 1981, *Ap. J.*, **243**, 411.
Helou, G., and Salpeter, E. E. 1982, *Ap. J.*, **252**, 75.
Hogan, C. J., and Kaiser, N. 1983, *Ap. J.*, **274**, 1.
Kapranidis, S., and Sullivan, W. T., III. 1983, *Astr. Ap.*, **118**, 33.
Klypin, A. A., and Shandarin, S. F. 1983, *M.N.R.A.S.*, **204**, 891.
Kuhn, J. R., and Uson, J. M. 1982, *Ap. J.* (*Letters*), **263**, L47.
MacGillavry, H. T., Dodd, R. J., McNally, B. V., and Corwin, H. G., Jr. 1982, *M.N.R.A.S.*, **198**, 605.
Moody, J. E., Turner, E. L., and Gott, J. R., III. 1983, *Ap. J.*, **273**, 16.
Oort, J. H. 1983, *Ann. Rev. Astr. Ap.*, **21**, 373.
Palmer, P. L. 1983, *M.N.R.A.S.*, **202**, 561.
Peebles, P. J. E. 1982, *Ap. J.* (*Letters*), **263**, L1.
———. 1983, preprint.
Peebles, P. J. E., and Dicke, R. H. 1968, *Ap. J.*, **154**, 892.
Primack, J. R., and Blumenthal, G. R. 1983, preprint, University of California at Santa Cruz.
Shanks, T. 1979, *M.N.R.A.S.*, **186**, 583.
Soneira, R. M., and Peebles, P. J. E. 1978, *A.J.*, **83**, 845.
Tifft, W. G. 1980, *Ap. J.*, **239**, 445.
Valdes, F., Tyson, J. A., and Jarvis, J. F. 1983, *Ap. J.*, **271**, 431.
West, M. J., and Dekel, A. 1984, in preparation.
White, S. D. M., Frenk, C. S., and Davis, M. 1983, *Ap. J.* (*Letters*), **274**, L1.
Zel'dovich, Ya. B. 1970, *Astr. Ap.*, **5**, 84.
Zel'dovich, Ya. B., Einasto, J., and Shandarin, S. F. 1982, *Nature*, **300**, 407.


AVISHAI DEKEL and MICHAEL J. WEST: Department of Astronomy, Yale University, New Haven, CT 06511

SVERRE J. AARSETH: Institute of Astronomy, Madingley Road, Cambridge CB3 0HA, England, UK